Chapter 1

Support Structure Design for Selective Laser Melting Process

Behzad Rankouhi[1], Dan J. Thoma[1,2,3], and Krishnan Suresh[1]

1 *Mechanical Engineering Department, University of Wisconsin-Madison, USA*

2 *Grainger Institute for Engineering, University of Wisconsin-Madison, USA*

3 *Materials Science and Engineering Department, University of Wisconsin-Madison, USA*

1.1 Introduction

It has been almost twenty years since the first metal-based powder-bed system was introduced to the world by EOS® in early 2000's. Before the advent of these systems, polymer-based sintering machines, also known as selective laser sintering (SLS) machines, were the only powder-bed systems in existence. In a way, SLS is the backbone of today's selective laser melting (SLM) systems. These SLM machines were part of the new generation of additive manufacturing systems that were the result of more than ten years of experience in producing polymer-based sintering machines [34]. Figure 0.1 illustrates the SLM process. Although the details of the process can vary slightly, the governing principles of the process remain the same, i.e. layer-wise melting of the powder bed by a laser beam.

SLM opened a window to new possibilities in design and manufacturing of metallic parts that we are still exploring. Ability to produce parts with high complexity and precision, competitive mechanical properties, and a wide selection of materials are the main advantages of this additive manufacturing process. In SLS, polymer powder is sintered to create a solid object. Sintering is the process of heating the powder to temperatures slightly below material's melting point to allow solid state diffusion and bonding of particles. On the other hand, in SLM process, metal powder is melted to create the object. Melting is the process of heating the powder to or above the material's melting point to allow formation of melt pool and fusion of powder particles across grain or particle boundaries. It is the formation of melt pool in SLM process that makes all the difference. Complications in the design of support structures – the main topic of this chapter – for SLM is mostly due to formation of this melt pool.

Unlike SLS where the loose powder provides sufficient support for the part, SLM requires additional support structure to secure the part on the substrate, support the weight, and reduce the temperature gradient of the part by transferring the heat of the melt pool to the substrate. Any surface with a normal angled at or greater than a specific range with respect to the build axis (Z axis in Cartesian system is commonly assigned to the build direction) requires a support structure. It should be noted that this *overhang angle* is material dependent. For SS316L, a common material used in SLM, the overhang angle is around 45°. Lighter metals with lower melting point in powder form will allow for slightly larger overhang angles. For consistency, we choose SS316L as the material of choice throughout this chapter. The need for support structure is arguably one of the major drawbacks of SLM process. Considering the overhang angle, one can see how addition of support structures brings about more complications to the design process. Orientation of the part, and location of the support with respect to the part become crucial factors when setting up a build [9]. More support structure means more material and energy consumption. Moreover, unsuitable support structure design can cause part failure, which in turn can lead to higher cost per part. Therefore, an optimum support structure design is critical for the SLM process.

An essential purpose of support structure in SLM process is transferring heat from the part to the substrate, therefore reducing the temperature gradient of the part during the manufacturing process. Smaller temperature gradient corresponds to lower residual stresses in the part which are the primary cause of deformation and warping. The secondary purpose of support structures is maintaining the surface quality of the part by preventing undesirable physical phenomena such as dross. Figure 0.2 shows an example of a typical support structure generated for SLM process that meets these requirements. Based on the role that support structures play in design process, it is evident that solely geometrical design solutions will not adequately address the problem; a comprehensive understanding of the physics of SLM process is required. Nevertheless, most of the solutions provided for support structure design for SLM are based on geometry and simplified physics [16, 22, 28]. The reason we tend to overlook the influence of physics of melt-pool perhaps stems from our relatively good knowledge of Fused Deposition Modeling (FDM) or desktop 3D printing process. To design support structures for FDM, we do not need to consider the heat transfer in the part, as a result the problem simply becomes a geometrical-structural design problem, and there are numerous solutions provided for design of support structure for FDM process [17, 21, 31]. Consequently, we are biased toward these designs that neglect the effects of heat transfer and melt pool formation. Therefore, while these solutions look elegant on paper, they cannot be regarded as designs that meet SLM requirements.

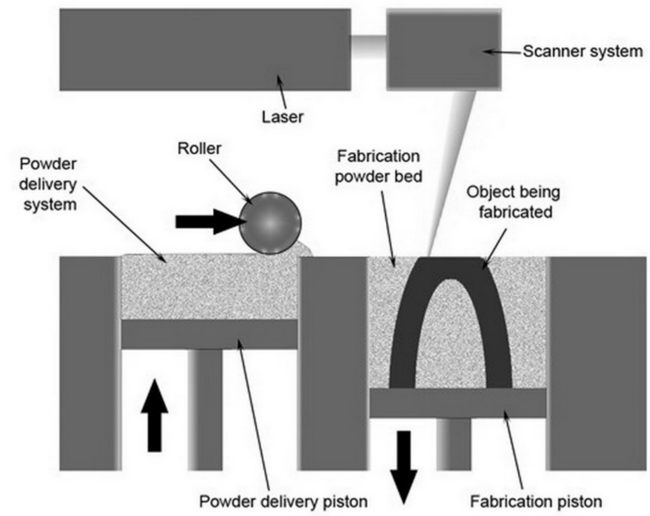

Figure 1: Graphical representation of SLM process. Some systems allow for more than one laser or reflective mirrors and some use blades instead of rollers to lay down a layer of powder [43].

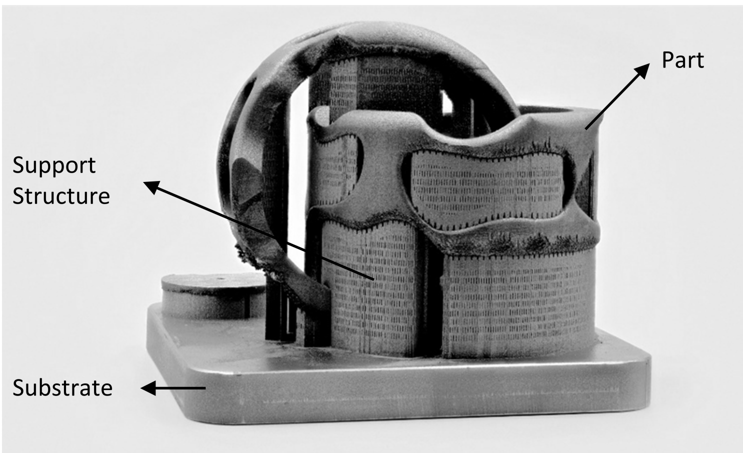

Figure 2: Stainless steel 316 object manufactured using SLM process. All overhanging surfaces are supported by a common support structure called block support (adopted from [18]).

Conceptually, support structure design for SLM lies at the intersection of three independent requirements, see Figure 0.3. First, we must understand the limits of manufacturing with SLM process. For example, what is the smallest achievable thickness or diameter? In other words, we must verify if our support structure design is *manufacturable*. Second, we must choose a support geometry that possesses enough *structural integrity* to be able to support the overhanging surfaces while being efficient in terms of build time and material consumption. Finally, and most importantly, the support structure should maximize the rate of *heat transfer* from melt pool to the substrate. Any support structure design that does not adequately address these three requirements, is not a suitable design for the SLM process.

In this chapter we aim to provide an overall view of support structure design for SLM. We start by defining the vocabulary that will be used to describe different aspects of a support structure. Then, we explore the metrics that should be considered when designing support structures. These metrics will provide a base line for comparing the effectiveness of different type of designs. Furthermore, we investigate conventional and novel designs. We explore the advantages and disadvantages of each design and provide examples. Finally, we discuss the possible directions where support structure design can take in the future.

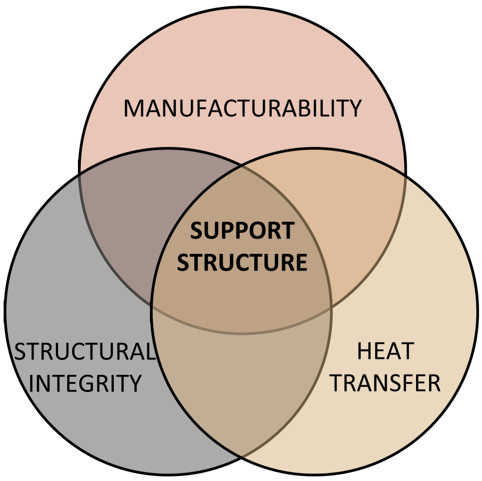

Figure 3: Support structure design for SLM cannot be addressed without considering three main requirements that govern the design process.

1.1.1 Support Structure Nomenclature

Before we delve into support structure design, we need to establish terminology that defines different features of a support structure. These are features that are common among most types of support designs. Features that are specific to a particular type of support structure will be defined in the designated section for that support type.

As mentioned in the introduction section, surfaces with normals that are oriented at or greater than a specific angle with respect to the build axis are called *overhang surfaces* and the specific angle is called the *overhang angle*. The overhang angle is material dependent and is determined experimentally. It is worth mentioning that in SLM process, parts are typically placed a few millimeters above the substrate which means that parts will be printed on a support structure and not directly on the substrate. This makes removing the part from the substrate more convenient, because a support structure is not nearly as dense as a solid part. However, there are exceptions where placing the part directly on the substrate proves to be advantageous. These scenarios are mostly dictated by the geometry of the part.

The subset of the support close to the part is of special interest. It determines the main functionalities of the support structure and it typically has a more complicated design compared to rest of the support structure. Therefore, we propose the body and comb concepts to better understand and distinguish between these two regions. Figure 0.4 shows a part together with a typical support structure. The support structure consists of two segments which serve different purposes. *Support body* refers to the larger segment of support structure which usually starts from the substrate and ends close to the overhang surface of the part. In addition to supporting the weight of the part, support body is responsible for transferring the heat from the part to the substrate, ensuring reduced temperature gradient within the part. *Support comb* refers to the upper segment of support structure where support and part meet. Support comb design plays a crucial role in the surface roughness of the part, ease of support removal, heat transfer, and overall success of the design. In scenarios where the part contains surfaces overhanging itself, support structure can contain two support comb segments and a connecting support body. This special case is depicted in the upper section of Figure 0.4.

From a CAD perspective, support structures can be represented as solids or surfaces. *Solid supports* are designs that contain a volume, while *surface supports* are designs with zero volume. Figure 0.5 shows two examples of solid and surface designs. In the cone design (left), each support occupies a volume (solid design). On the other hand, in the web design (right), the support is represented as a surface (the thickness will be implicitly assigned through process parameters). We will take advantage of this distinction later in the chapter where we introduce support structure metrics.

Finally, some designs are *open structures*, i.e. there is no border wall surrounding the structure. The cone design in Figure 0.5 is an example of an open structure. On the other hand, *closed structures* are structures with a surrounding wall, such as the web design in Figure 0.5. Open structures allow for the un-melted powder to escape while closed structures trap the un-melted powder inside. The trapped powder can only be removed after the part is separated from the substrate. We will revisit the concept of open and closed structures when we introduce the metrics in support structure design.

1.2 Support Structure Metrics in SLM

Before we can discuss metrics to gauge support structure performance, we briefly review the governing physics of the problem that is dictated by the melt pool. There are various characteristics associated with melt pool in SLM, among them, temperature and size are the most influential in support structure design. The two most important parameters affecting the temperature and size of the melt pool

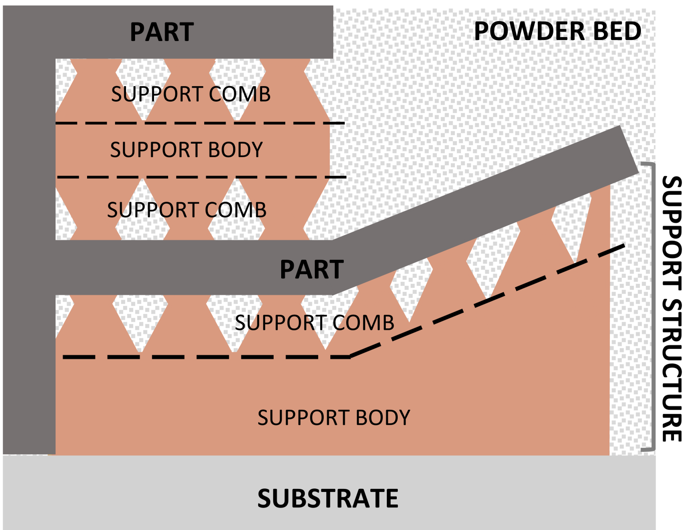

Figure 4: Support structure segments. The design strategy and requirements for each segment is unique to the type of support structure.

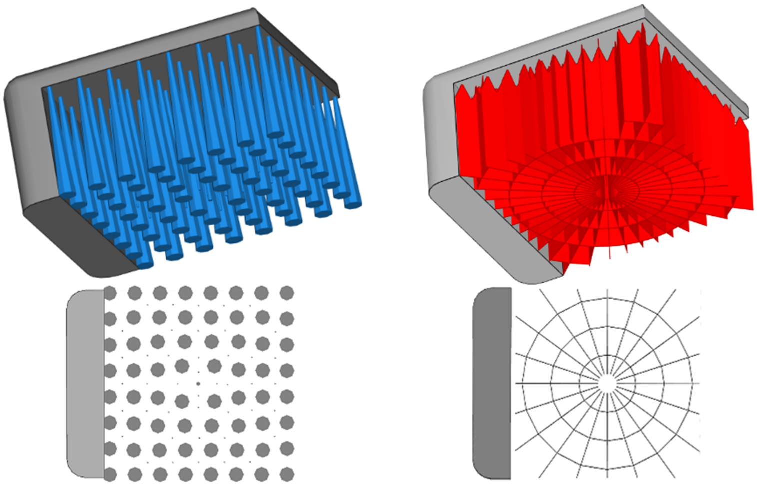

Figure 5: Cone design (left) is an example of solid support design, and web design (right) is an example of surface support design.

are laser speed and power. Often, these are combined into a single parameter: *linear energy density (LED)* defined as [36]:

$$E_L \approx \frac{P}{v} \tag{0.1}$$

where E_L is linear energy density in *J/mm*, P is laser power in W and v is laser speed in *mm/sec*. In practice, surface oxide, reflectivity, plasma, vaporization, etc., all affect the effectiveness of the linear energy density.

Temperature of the melt pool increases significantly by increasing the laser power or decreasing the laser speed. Melt pool temperature is in the order of thousands of degrees Celsius and it depends on the material's melting point in powder form and powder particle shape and size distribution. Dimensions of the melt pool are also a function of laser power and speed and they are in the order of hundreds of micrometers. Figure 0.6 shows a simplified drawing of melt pool dimensions in SLM process. Length, width, and depth of the melt pool increase with an increase in LED or laser power. However, an increase in laser speed alone will reduce the width while elongating the melt pool [29, 37].

Next, we consider the relationship between these two melt pool characteristics and design of support structure features. We discuss the defects that a proper support structure can help prevent and establish the metrics that are common between all support structure types.

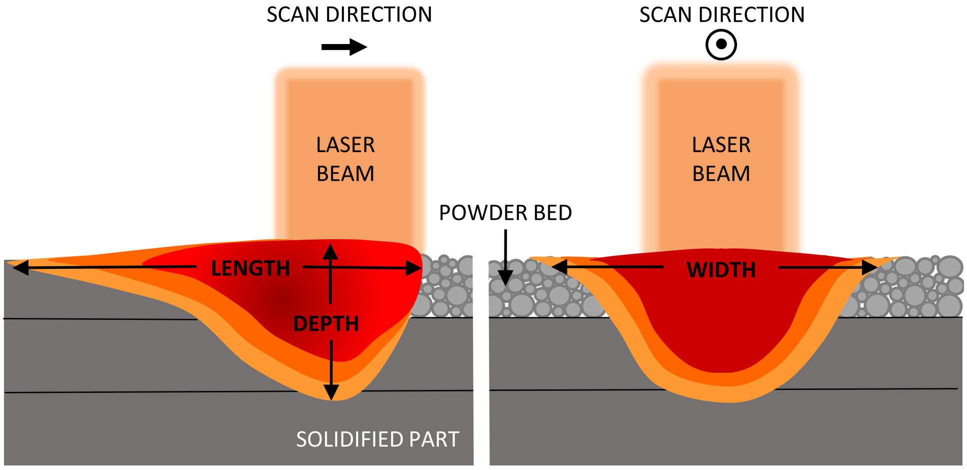

Figure 6: Simplified schematic of melt pool dimensions and shape in SLM.

1.2.1 Part Quality

The first metric in support structure evaluation is part quality. This metric measures the quality of the manufactured part after the removal of support structure. There are certain defects that can affect the quality of the part that an effective support structure can prevent.

Residual stress induced defects

Residual stresses are stresses that remain within the part after the manufacturing process is completed and the part is in equilibrium with its environment. It is an inherent consequence of SLM process. These stresses can cause warping, delamination, distortion, and cracking [7].

(1) *Warping* is defined as plastic deformation due to thermal stresses caused by rapid solidification of the part [32]. This plastic deformation occurs when the thermal stresses exceed the yield strength of the material. Therefore, it is more likely to happen in regions with thin features or overhangs, where each layer is slightly shifted forward, resulting in a small thin surface (Figure 0.7). Moreover, the staircase effect of SLM process exacerbates the warping issue. As shown in Figure 0.7.a, deflection of each layer accumulates as consecutive layers solidify, causing the last layer to protrude the powder bed. If this protrusion exceeds the layer thickness, it collides with the recoater blade when a new layer is being deposited, causing the entire build to fail. The reason the thermal stresses exceed the yield strength of the material in overhang surfaces is that heat from the melt pool does not transfer to the substrate which acts as a heat sink. It is expected that thermal

conductivity of a metal in powder form is approximately 100 times lower than its solid form [24], as a result, the absence of support structure, means that the generated heat stays in the part to cause high thermal stresses.

(2) *Delamination and cracking* is defined as separation of two consecutive layers due to residual stresses. Similar to warping, delamination occurs due to high stresses at the layer interface [23]. Figure 0.8 shows examples of defects caused by residual stresses.

Physical phenomena responsible for the origin of residual stresses are still being investigated. High temperature gradient within the part due to traveling melt pool, thermal expansion/contraction and non-uniform plastic deformation are the main factors in accumulation of residual stress in the part [7, 29]. In addition, an inadequate support structure can aggravate this intrinsic consequence of SLM process.

It should be noted that utilizing support structure is not the sole remedy for the above-mentioned defects, nor will it fully prevent the occurrence of these defects. There are other contributing factors, such as change in process parameters that can help with residual stress induced defects. Some examples of other remedial approaches include: (1) reducing layer height to minimize the staircase effect which can lead to reduction in warping, (2) increasing the substrate preheat temperature to reduce the temperature gradient in the part which can lead to lower

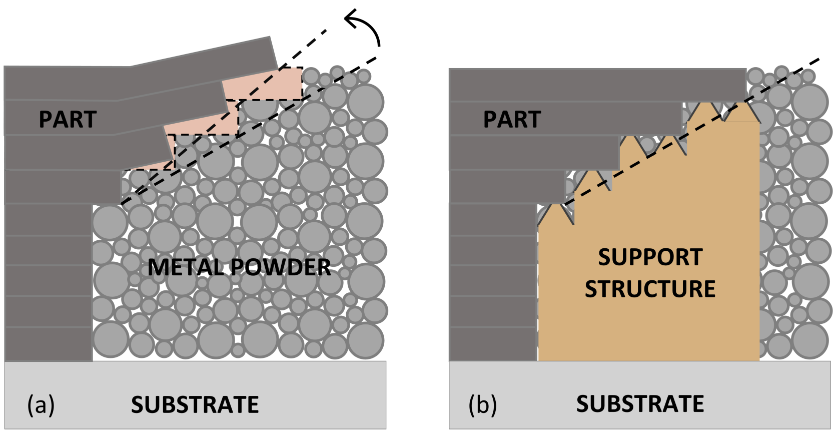

Figure 7: (a) Warping in an unsupported overhang surface. (b) An effective support structure can prevent warp from happening.

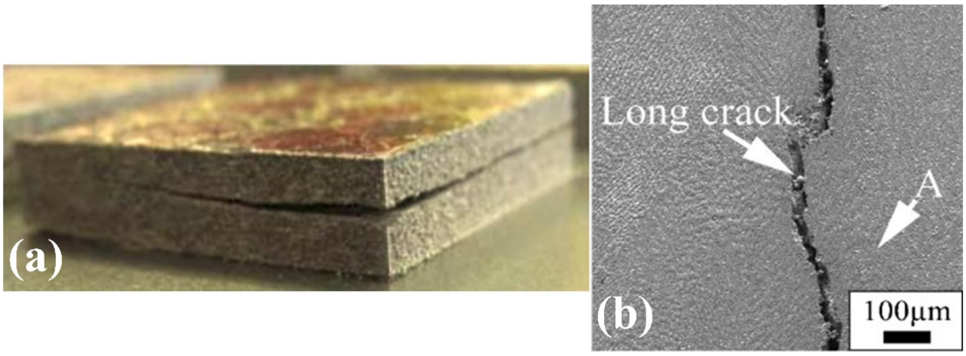

Figure 8: (a) Delamination at layer interface during cooling [14]. (b) crack formation in heat affected zone [40].

thermal stresses, and (3) controlling the process parameters of SLM; for example, shorter laser scanning vectors or island scanning patterns, increase in scanning speed, and increase in powder bed temperature have shown to reduce distortion and residual stresses in the part [2, 26].

Dross

This defect is defined as unintentional partial or complete melting of powder particles below the current layer. As explained earlier, during melting an overhang surface with no support structure, the heat conduction rate is very slow. Therefore, the absorbed energy of powder bed will be much higher resulting in much larger and heavier melt pool. Rayleigh-Taylor instability in the gravity field along with capillary forces will cause the melt pool to sink into the powder bed. Dross will form when the heat from the sunk melt pool causes unintentional melting of surrounding powder particles [3, 6, 8]. As shown in Figure 0.9, dross can affect the top surface of the overhanging layer as well. Severe dross will cause high surface roughness on top of the overhanging layer which in turn can lead to build failure if the recoater collides with the uneven surface.

Presence of support structure underneath the overhanging layer prevents melt pool enlargement and sink into the powder bed. Further, it is important to note that the gap between each tooth of support comb is directly related to the melt pool size. If this gap is too large, the melt pool will have enough space to grow and form dross. This is one of the main reasons why an effective support comb design is crucial in preventing dross.

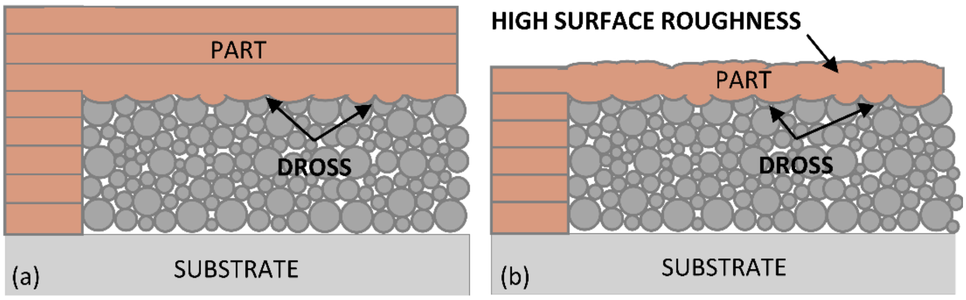

Figure 9: (a) Dross formation in the absence of support structure. (b) Sever dross can cause high surface roughness on top of the overhanging layer causing failure of the entire build.

1.2.2 Support Material Volume

Another important metric in assessing support structures is its volume. Between two different support structures with identical performance, the one with lower volume is preferable. There are however two important observations to make.

First, recall that a support structure can be represented as a solid, or a surface with process-dependent thickness. Figure 0.10 shows the two different support structure representations. In the former, the volume is easily computable from the CAD geometry. In the latter, the thickness is determined by laser power and speed that can be combined into a single parameter: *planar energy density* (PED) defined as:

$$E_P \approx \frac{P}{v.t} \tag{0.2}$$

where E_P is planar energy density in *J/mm*^{2}, P is laser power in W, v is laser speed in *mm/*sec, and t is layer thickness in *mm*. Higher PED's will result in slightly thicker supports. For example, for SS316L, PED of 0.15 *J/mm* will result in wall thickness of ~0.12 *mm* while PED of 0.19 *J/mm* will result in wall thickness of ~0.15 *mm*.

The second observation is that for a given volume of support, the material consumed (i.e., the weight of the support) is once again process dependent. If the laser power per unit volume is low, then there will be incomplete melting of powder particles, leaving pores inside the material. This leads to lower density of the support structure and reduced material consumption [27]. A typical process parameter used to evaluate full/incomplete melting is the *volumetric energy* *density* (VED), defined as the average applied energy per volume of material during the scanning of one layer [27, 30]:

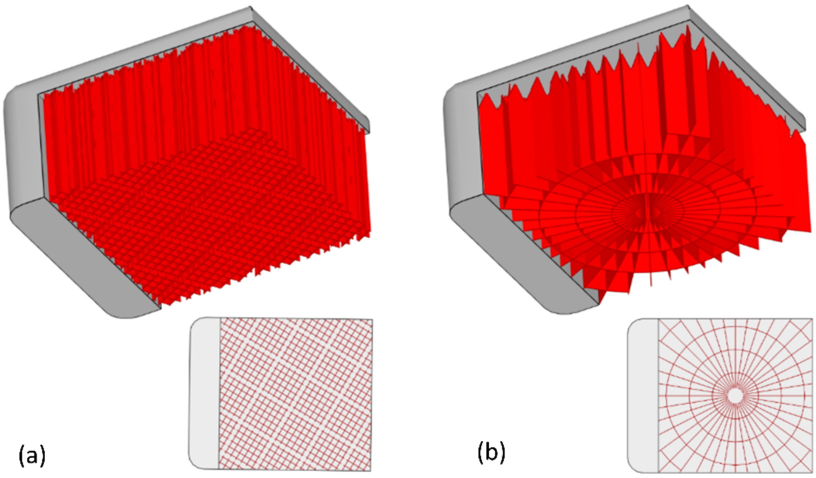

Figure 10: (a) Block support structure. (b) Web support structure. Given the same process parameters, the web design has 42% less volume.

$$E_V \approx \frac{P}{v.h.t} \tag{0.3}$$

where E_V is volumetric energy density in J/mm^3, P is laser power in W, v is laser speed in *mm/*sec, h is hatch distance in *mm*, and t is the layer thickness in *mm*. Choosing different laser power, laser speed, layer thickness or hatch distance can result in different density or fill-ratio.

1.2.3 Support Manufacturability

This brings us to our next metric in support structure design, manufacturability of the support structure. The first rule ironically states that the supporting structure should be self-supporting, both in terms of overhanging surfaces and its susceptibility to defects. We know that defects such as distortion due to residual stresses can be caused by excessive absorption of energy by the powder bed. Therefore, support structure immunity to defects is tightly tied to process parameters, especially VED and PED. To understand how these two parameters can affect the manufacturability, we need to revisit the representation of support structures, namely, solids and surfaces. Most common designs fall in the surface category, such as the designs shown in Figure 0.10. In these designs, every feature of the model is a surface, therefore there is no infill scan strategy, there is only single scan vectors. For this group of support structures, PED is the important process parameter. On the other hand, designs such as the cone (Figure 0.11), contain solid features that require infill scan strategies. In other words, we should consider hatch distance, hence the VED becomes the important process parameter for this group of supports. Now, we can apply the same concepts that we introduced before regarding melt pool, residual stress and defects, to support structure manufacturing.

Consider the scan strategies for solids and surfaces. Figure 0.12 shows a cross sectional view of tree and block support structure designs. Movement of a laser beam is depicted by an arrow which we call a *scan vector.* These vectors inform us of *direction* and *orientation* of laser beam's movement. In the surface representation, there is a single laser beam pass, i.e., a single scan vector, for each wall segment, whereas for a cone design, multiple passes of laser beam are needed to create a solid geometry.

Figure 0.13 shows a failed lattice support structure as an example that highlights the importance of manufacturability metric. In this design, lattice strut diameter was set to 0.1 mm. Coincidentally, the machine that manufactured the part had a minimum feature size of 0.1 mm. Therefore, although the support structure in this example is represented as a solid, there is no room for any infill scan strategies. In scenarios such as this, using VED will apply excessive energy to the powder bed which can cause lattice strut deformation. In Figure 0.13 deformed struts protruded the powder bed and collided with the recoater. Accumulated deformation finally destroyed the entire support structure leaving the overhang surface of the part unsupported. Finally, severe dross and instability led to failure of the entire part. To avoid failures such as this, one can treat a solid representation as a surface representation, and use appropriate process parameters such as PED.

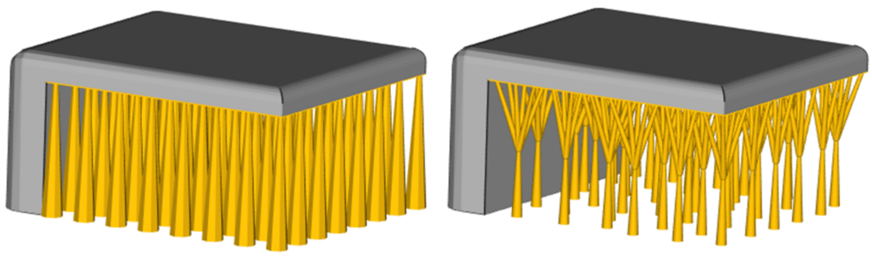

Figure 11: Cone (left) and tree (right) support structure design. Both designs are examples of 3D solid designs.

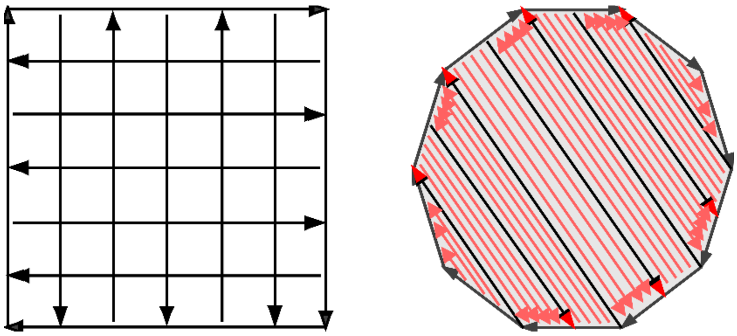

Figure 12: Cross sectional view of a block design and its scanning vectors (left), and a single cone of a cone design and its scanning vectors (right).

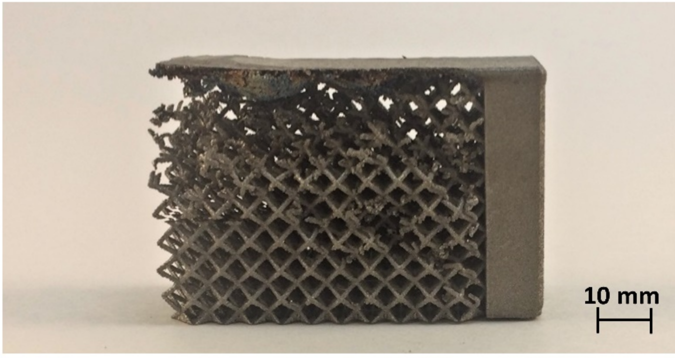

Figure 13: Using improper process parameters caused the lattice support structure to fail which led to the failure of the entire build. This example highlights the importance of manufacturability metric in support structure design.

1.2.4 Post processing and removal

The final metric in support structure design is the ease of removal, and required post processing steps. Removing support structure is a tedious task, and it is usually done manually. A support structure design that expedites removal is greatly beneficial. But support removal is not the only post-processing concern. During the manufacturing process, unused powder can get trapped inside the support structure. Further, since the structure is usually enclosed by the substrate at the bottom, and the part at the top, this trapped powder cannot be released unless the part and its support structure is removed from the substrate. Since removal is typically done by means of electric discharge machining (EDM), or use of power saws, the released trapped powder becomes contaminated and not reusable. For large parts and high production rates, loss of trapped powder can harm the economics of SLM process.

To reduce support removal time, effective support comb designs are required. Figure 0.14.a shows an example of a lattice support structure with an effective comb design that can be easily removed using simple hand tools while Figure 0.14.b shows an example of a support structure that is impossible to remove without the use of power tools due to lack of support comb structure.

Few attempts have been made by researchers to automate or expedite the removal process. In one study, Lefky et al.[18] attempted to automate the support removal process by using self-terminating electrochemical etching. They incorporated a sensitizing agent during the heat treatment process to chemically destabilize 100-200 μm of the part's surface. The part is then etched with a high selectivity toward the sensitized surface over the substrate. The etching process self-terminates when the sensitized layers are removed. This approached proved to be effective for 17-4 PH stainless steel and SS316L. Figure 0.15 shows the proposed removal process applied to a SS316L part with a complex geometry. It should be noted that during this process 120 μm of the part were removed along with the support structure.

In another study, Wei et al. [33] demonstrated an easy-to-remove support structure for SS316L made with SiC-SS316L composite. The composite material with 40% volume fraction and 320 grit SiC produced enough mechanical defects during the SLM process that the transition zone between part and support was easily broken by applying a low external force. Addressing cross-contamination and high surface roughness proved to be challenging in the proposed method. Figure 0.16 shows a simple overhanging surface that is supported by SiC-SS316L composite support structure.

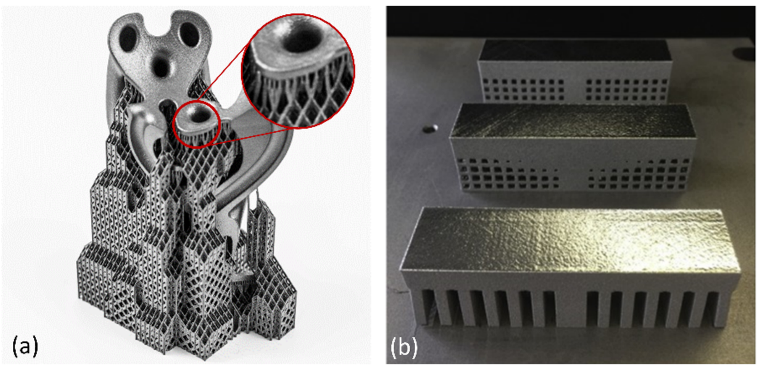

Figure 14: (a) An example of a lattice support structure with effective comb design. Removal of this support structure is relatively simple [41]. (b) An example of support structure with no comb design. It is impossible to remove this support structure without extra machining [4].

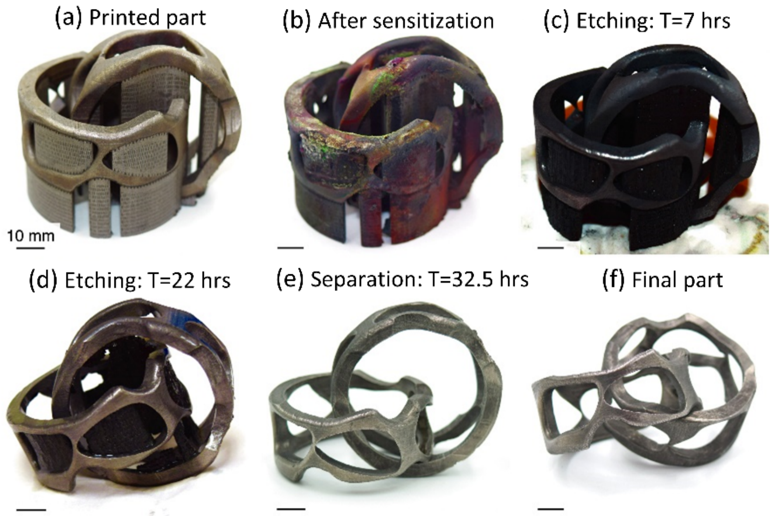

Figure 15: Support structure removal using electrochemical etching applied to SS316L. The geometry of the part is mostly preserved after 33 hours of etching and support material removal [18].

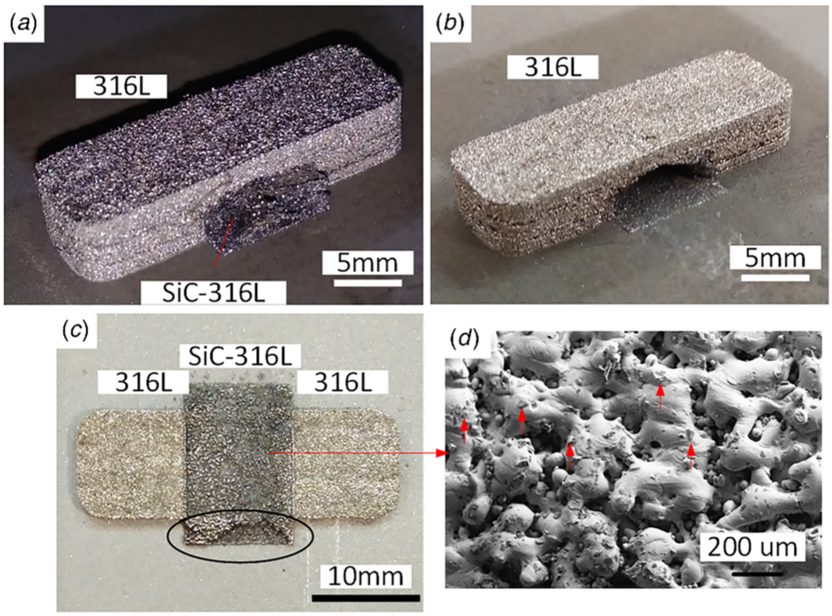

Figure 16: (a) A bridge structure using SiC-316L as the support material at the aperture position, (b) the support structure removed, (c) cross section of the bridge structure, and (d) the SEM image of the top surface of the laser sintered SiC-316L support structure [33].

Although these efforts show great promise, they remain highly material dependent and cannot be widely applied. Today, most support removal is still done manually, therefore there is no proper way of quantifying this metric. Support removal will remain a qualitative metric for assessing different type of support structures.

On the other hand, trapped powder is quantifiable. Consider the closed support structures in Figure 0.10. The actual support volume is the volume of the support structure plus the volume of the trapped powder, whereas in an open support structure (see Figure 0.11), the actual support volume is the same as the volume of the support structure. To mitigate the trapped powder problem, use of open structures is recommended. Further, there are some approaches that will allow closed structures to release the entrapped powder. We will discuss this feature in the next section.

1.3 Support Structure Design and Manufacturability

In the previous section, we introduced certain metrics for evaluating support structure designs. In our view, any design that is part of this landscape is an acceptable design. Some might be more effective, robust, or efficient than others. This section is dedicated to introducing existing support structure designs. We will start by discussing conventional designs that are industry standards. Later we introduce novel designs, and discuss their advantages and disadvantages.

1.3.1 Conventional Support Designs

Conventional support structure designs are the most robust and widely utilized designs in the industry today. They are not optimal structures in terms of material consumption or build time, but they are the most reliable. Unfortunately, there is no universal terminology to compare these designs and define their features. Therefore, we adopt the terminology from Materialise® Magics®, an industry leading data and build preparation suite for AM [42]. Based on this terminology, the conventional support designs include: block, web, contour, line, gusset, and point. We introduce the block design and its features below. The remaining, are variations of the block design, created to accommodate certain geometrical scenarios. We will briefly discuss these scenarios, but readers are referred to commercial support generation packages for further details.

Block design

Arguably the most widely used, and reliable support structure design, is the block design. It consists of zero-thickness walls that are arranged to form a grid, and it is suitable for large overhang surface areas; see Figure 0.10.a. Main advantages of block design are good manufacturability and high heat transfer rate. Its shortcomings are high volume, and difficulty in removal. Figure 0.17 shows a schematic of the block design grid. Critical dimensions of the grid are defined in Table 0.1. These values are material dependent and are determined experimentally.

Hatch distances are critical in preventing dross, and they depend on the melt pool characteristics. Moreover, they correlate to the relative density of the structure which in turn determines the heat transfer rate of the support structure. If the hatch distances are too large, dross will form within each block of the grid, and residual stresses will increase due to low heat transfer rates. On the other hand, small hatch distances will unnecessarily increase the support volume and hinder support removal. The *separation width* is another critical dimension that helps ease support removal by fragmenting the grid.

The next feature within the support body is *perforation*, see Figure 0.18 and Table 0.2. Perforation allows trapped powder retrieval. Perforations are usually

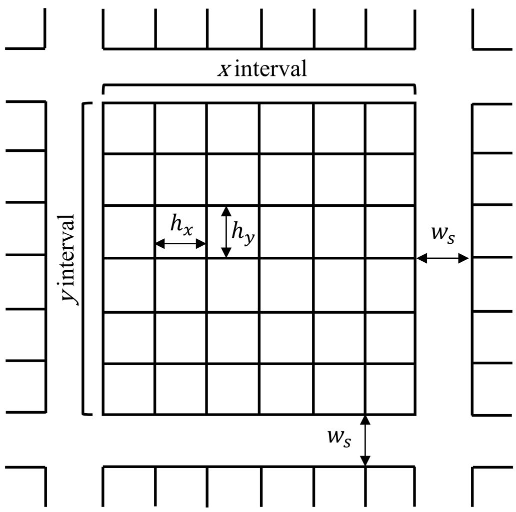

Figure 17: Grid schematic of the block support structure design and its critical dimensions.

diamond or rectangle shaped. Although they turn the block design into an open structure, some trapped powder will still remain inside the support structure. Making the perforations larger can cause build failure [3].

Table 1: Critical dimensions and their description for a grid in block design.

Dimensions	Description
h_x	Hatch distance in x direction.
h_y	Hatch distance in y direction.
x interval	Number of squares in x direction for each block.
y interval	Number of squares in y direction for each block.
w_s	Separation width which determines the fragmentation distance.

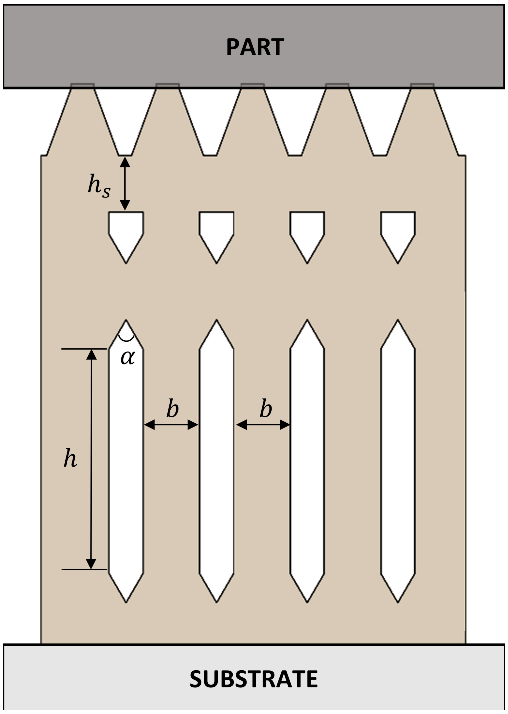

Figure 18: Schematic of perforations and critical dimensions in block support structure design.

Table 2: Critical dimensions and their description for perforations in block design.

Dimensions	Description
h_s	Solid height, distance between the last perforation and support comb or first perforation and substrate.
h	Height of the diamond perforation.
α	Angle of the diamond perforation.
b	Distance between each perforation, known as beam.

Figure 0.19 shows the support comb for the block design. Critical dimensions are defined in Table 0.3. This comb design facilitates the removal of support structure. Moreover, it ensures that the surface quality of the part is within acceptable range. Perhaps the most critical dimension in support comb is Z_{offset}, the amount of support penetration into the part. A common rule states that Z_{offset} cannot be smaller than the thickness of two layers. This ensures adequate support-part fusion.

Figure 0.20 shows different views of block support structure, manufactured using SS316. Figure 0.20.a reveals perforations on the border wall of the support structure. Figure 0.20.b gives a clear view of hatch intervals and fragmentation of the blocks, and Figure 0.20.c illustrates the support comb. Observe that the manufactured comb bears little resemblance to the design in figure 0.16. The reason is that critical dimensions of support comb are in the order of hundreds of microns which is in the same order as powder particle size. At this scale, model's geometry cannot be fully preserved during manufacturing, but the resulting structure can still alleviate support removal.

Recommended values for critical dimensions of the block design are provided in Table 0.4. These are conservative values to ensure a successful build. Different values for most cases are permissible but it requires experimental validation. It is important to note that these numbers are validated for a particular SLM machine and a particular metal powder vendor. Observe the subtle differences in critical dimensions for each material. These differences are driven by machine's laser and optics and melt pool characteristics.

Other conventional designs

Other conventional designs are similar in concept to the block design. Support body and support comb serve the same purpose as in block design. Perforations and fragmentation can be implemented in support body while the same comb design can be used for every design. Instead of grids, surfaces are arranged to form different patterns to better accommodate different geometries.

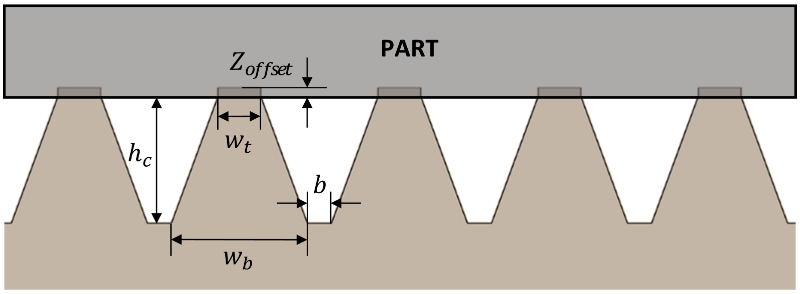

Figure 19: Support comb and its critical dimensions for block design.

Table 3: Critical dimensions and their description for support comb in block design.

Dimensions	Description
h_c	Comb height.
w_t	Comb width at top of the comb structure.
w_b	Comb width at base of the comb structure.
b	Base interval.
Z_{offset}	Penetration distance of support comb into the part.

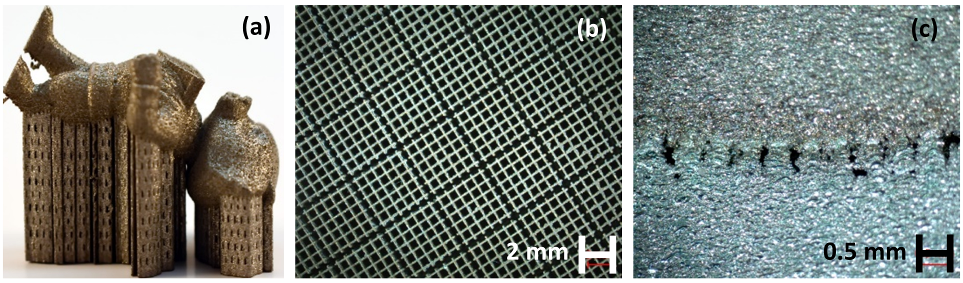

Figure 20: Three different views of block support structure, emphasizing on different features of the design.

For example, the *web design* is recommended for circular surfaces, due to its circular pattern. Users can change the number of ribs and circles based on the material (Figure 0.21.a).

Contour design is created by offsetting a pattern, repeated to cover the entire overhang surface (Figure 0.21.b). This pattern depends on the geometry of the overhang surface. Since there are no orthogonal surfaces intersecting the pattern to buttress the structure, this design is susceptible to build failures. On the other hand, it is easy to remove.

Line design is created for thin surfaces or edges, as shown in Figure 0.21.c. A single wall follows the path of the overhang surface and provide adequate support. Ribs can be added to the wall to provide reinforcement and decrease failure probability. One of the main disadvantages of this design is the likelihood of residual stress induced defects. This design is recommended for delicate parts such as small surgical instruments, where support removal can irreversibly damage the surface of the part.

If there is a small overhang surface far from the substrate in the build direction, gusset design (Figure 0.21.d) can be used to save time and material. The advantage of this design is its minimal volume and ease of removal. Gusset design takes advantage of the fact that the body of the part itself can be used as a

Table 4: Recommended values of block support design for popular materials. Adjusted for 400W Yb (Ytterbium) fiber laser [42].

Dimension	Recommended Value [mm]			
	SS316L	AlSi10Mg	Ti64	Inconel718
		Grid		
h_x	0.8	0.7	0.7	0.8
h_y	0.8	0.7	0.7	0.8
w_s	0.8	0.7	0.7	0.8
		Perforation		
h_s	0.5	0.254	0.254	0
h	2	1	1	0.6
α	60	60	60	25
b	0.6	1.2	1.2	0.4
		Comb		
Z_{offset}	0.04	0.03	0.03	0.12
w_t	0.2	0.2	0.2	0.2
h_c	0.6	1	1	0.8
w_b	0.7	0.6	0.6	0.6
b	0.1	0.1	0.1	0.1

heat sink. A compromise must be made between saving time/material and altering the thermal history of the part.

Finally, *point design* is meant for singular, small, and down-facing overhang surfaces as illustrated in Figure 0.21.e. Situations where a point design is required seldom occurs but when they do, using a point design help save time and material.

Currently, there are no tools available to automate the generation of different types of support designs based on the overhang geometry. Hence, choosing the appropriate support design and its critical dimensions rests on user experience.

1.3.2 Novel Support Designs

Besides conventional designs, researchers have also experimented with novel designs to improve on some of the metrics introduced earlier. In this section we will review some of the proposed designs.

Tree structures

Gan and Wang [8] proposed three different designs, shown in Figure 0.22. They concluded that an effective support structure should promote uniform heat dissipation and have a maximum for support comb spacing. Design (b) has more connection points compared to design (a) but the part experienced warping nonetheless. They hypothesized that the inclined connection points are the cause of warpage. Design (c) consists of an array of pin supports. Among the three proposed designs, design (c) yielded the poorest surface finish. A closer look at the manufactured examples in Figure 0.22 reveals the dross formation in all three designs. It is fair to say that although these designs performed well on support removal, manufacturability, and volume metrics, they performed poorly on part quality metric.

In another study, Zhang et al. [39] proposed a tree structure design (Figure 0.23) with the ability to change the branch diameter, angle, and number. They showed that their design can support large overhanging planes. Moreover, compared to conventional support structures, the proposed tree structure can save 23% on material and about 30% on scanning time. Although this design showed good performance on support volume, and manufacturability metrics, it did not perform well on post processing metric. Lack of support comb in this design compels the user to use excessive machining for support removal.

Lattice structures

From an engineering point of view, a lattice is defined as a pattern, known as a unit cell, which is repeated regularly in all directions. These light-weight structures have large surface area to volume ratio which provide them with good thermal dissipation property. These properties make lattice structures a potent candidate for support structures.

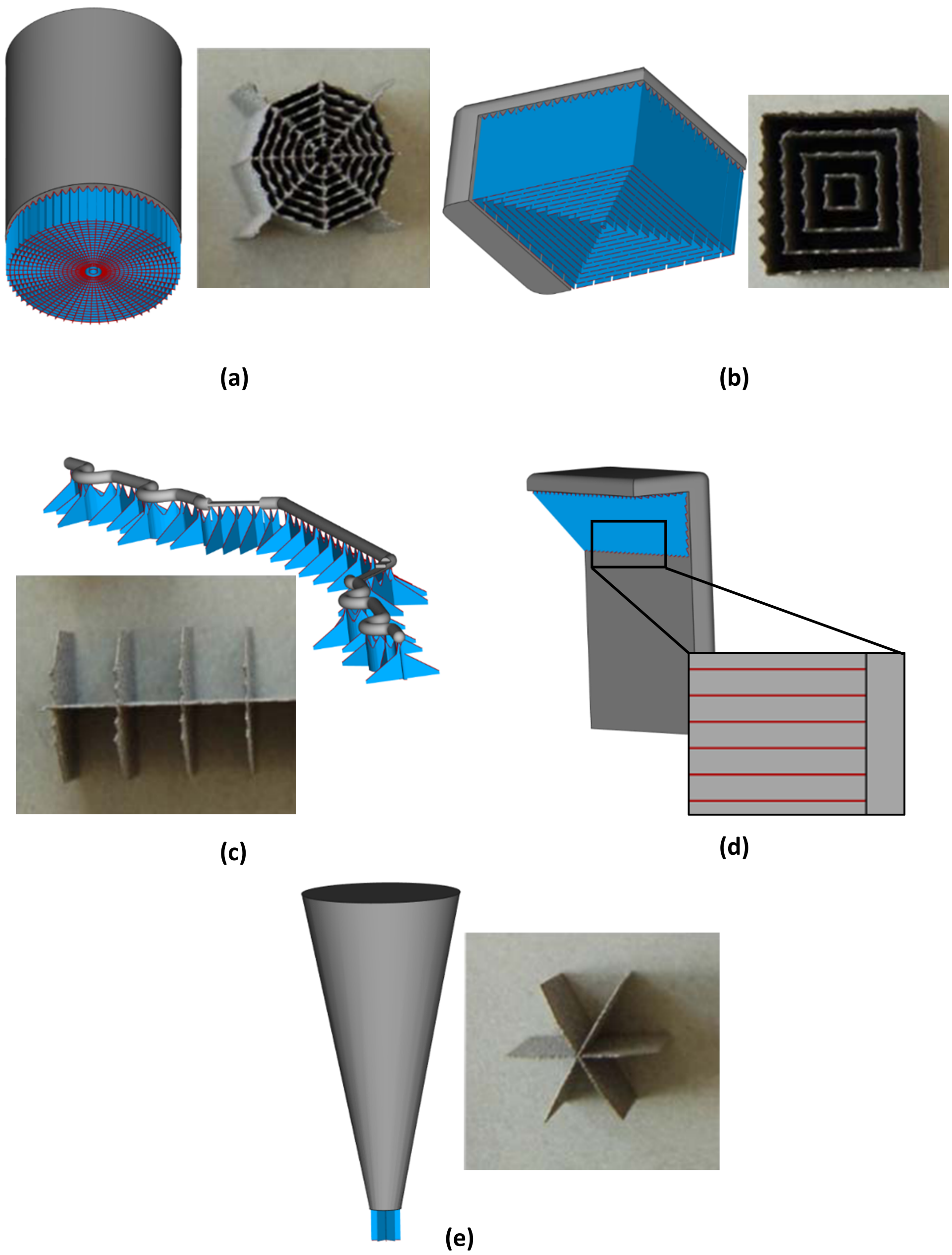

Figure 21: Conventional support structure designs and their corresponding cross sectional view as fabricated by SLM [13]. (a) web, (b) contour, (c) line, (d) gusset, and (e) point.

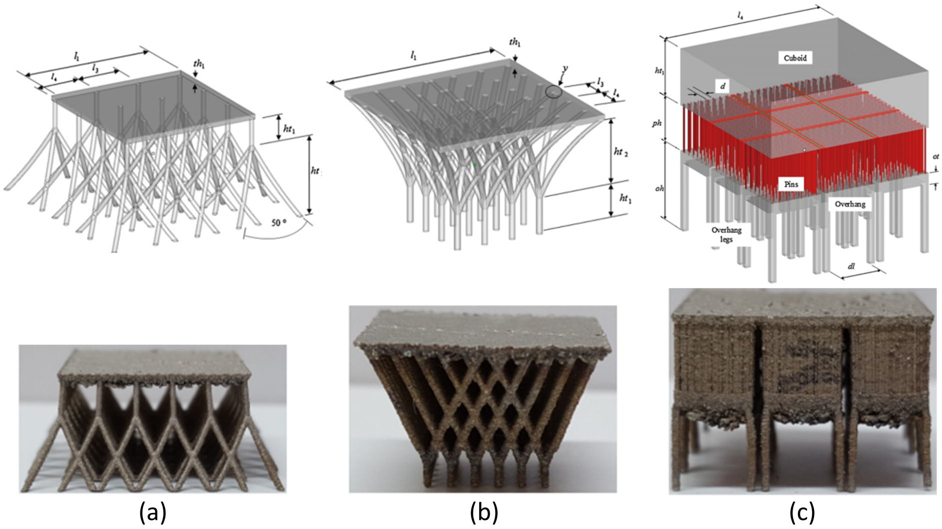

Figure 22: (a) Inverse Y design, (b) Y design, and (c) pin design. Proposed by Gan and Wang [8] as practical support structure designs.

Cloots et al. [20] studied a variation of BCC lattice structure with an emphasis on SLM process parameters. They were able to successfully implement their design and manufacture an overhang surface (Figure 0.24). High heat transfer rate of the structure helped prevent any residual stress induced defects. However, there was dross formation on the overhang surface. The advantages of this design are acceptable part quality, low volume, and ease of removal. Its drawback is in manufacturability. Authors reported that to successfully build the overhang on top of their support structure, they had to change the PED during the process resulting in part densities between 89.4% and 98.4%.

In another study, Hussein et al. [12] investigated two types of lattice support structures, Schwartz diamond and Schoen gyroid shown in Figure 0.25. They focused on openness of lattice structures and trapped powder retrieval along with build time for each design. They concluded that smaller cell sizes will result in longer print times and more material consumption. They achieved excellent part quality and support volume, but support removal was not considered in their study. Compared to other unit cells, diamond and gyroid created larger contact areas with the part. That means breaking the support structure from the part would be difficult.

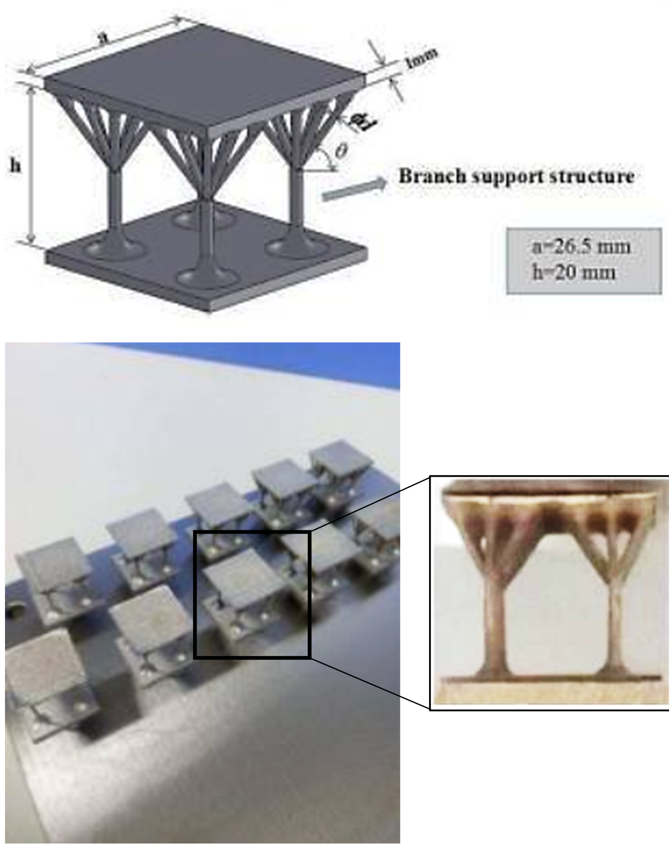

Figure 23: Tree (branch) support structure design proposed by Zhang et al. [39]. Manufactured by SLM from SS316.

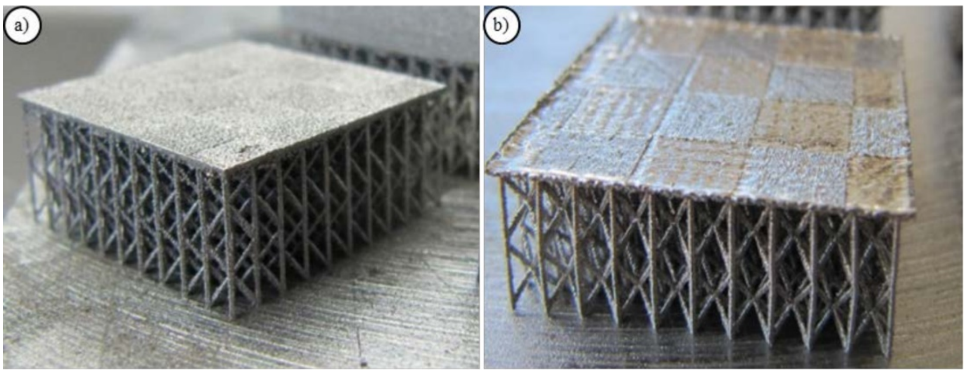

Figure 24: Lattice support structure made with SLM. (a) PED = 0.85 J/mm^2 and density of 89.4%, and (b) PED = 2.35 J/mm^2 and density of 98.4% [20].

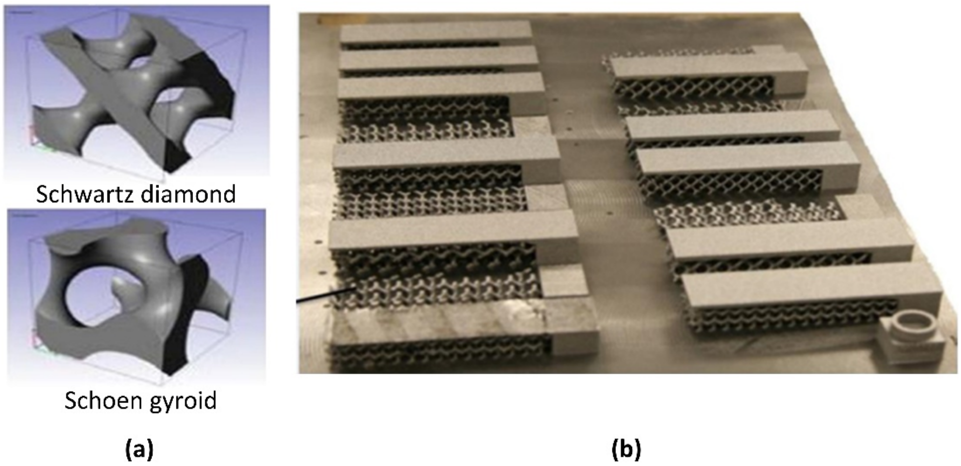

Figure 25: (a) CAD models of diamond and gyroid structures. (b) Manufactured cantilever parts and their lattice support structures [12].

1.3.3 Customized, Simulation Based Support Design

Both the conventional and novel support structure designs discussed above require the user to make critical decisions. Poor decisions can lead to build failure, or, at best, an inefficient design. With increased computational power and fundamental understanding of SLM physics, *we foresee an increase in use of simulation tools to create customized and optimized support structures*.

Numerous efforts have been made to simulate the SLM process at a micro scale, where laser interaction with powder, powder melting, and evolution of melt is considered [10, 35, 37, 38]. Other approaches are in the macro scale where laser heating and melting is treated as a thermal source, part shape, and laser scan strategies are taken into account, and residual stresses and local effective material properties can be calculated [1, 11, 19, 25]. The above-mentioned approaches are computationally expensive and they are not applied to the support structure. Only recently researchers tried to implement simulation based support structure design. For example, Cheng et al. [4] investigated the feasibility of using topology optimization in support structure design to mitigate residual stress induced defects. They used the inherent strain method for residual stress calculations during the SLM process to significantly reduce the computational cost of their approach. Variable density lattice structures were used due to their open design with the objective to minimize the mass of the support structure under stress constraints. Figure 0.26 shows the resulting design. They were able to reduce the weight of the support structure by 60% while mitigating cracking and warping induced by SLM process. Design shown in Figure 0.26 proved to satisfy all the metrics introduced in this chapter, except for ease of removal. The lattice structure lacks support comb to alleviate the removal process.

In another similar study [5], a voxel-based fictitious domain method is used to calculate residual stresses in the design domain which includes the support structure. This approach reduced the computation time and allowed for residual stress minimization through part orientation optimization based on process modeling. Moreover, the yield strength is computed using a multi-scaled model. Finally, a multi-objective optimization is carried out to minimize both residual stresses and support volume. Figure 0.27 shows the proposed method and support structure design. Similar to previous work, the proposed design performed well on all metrics except the ease of removal.

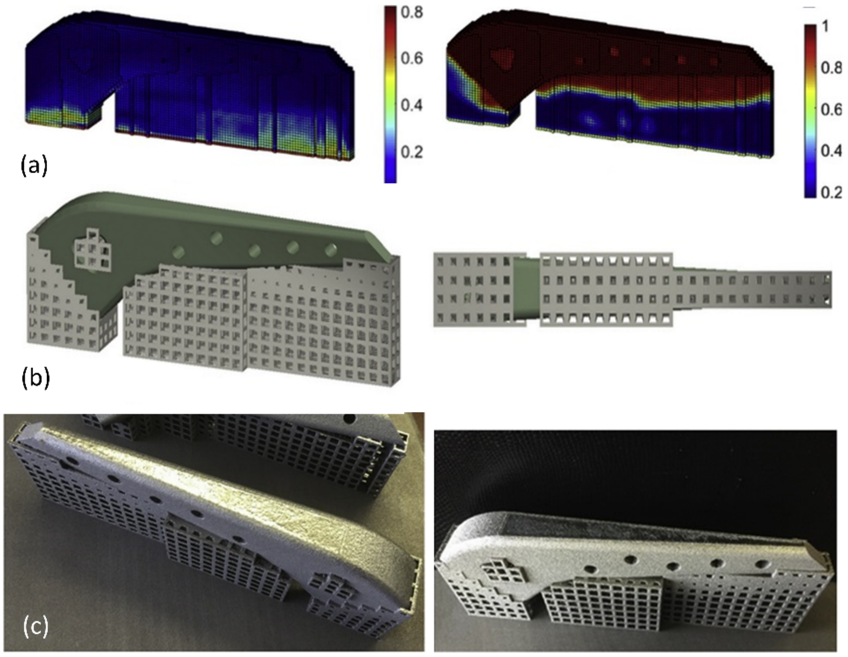

Figure 26: (a) Optimization results of normalized residual stress distribution in the model [4]. (b) Reconstruction of the optimal support structure design using variable-density lattice structure [4]. (c) Manufactured designs using SLM process and Ti6Al4V [4].

Based on the metrics introduced in this chapter, a simulation tool suitable for support structure design requires a multiscale modelling approach, wherein melt pool dimensions and temperature, and residual stress development in the part are both implemented [15], and coupled with support structure build simulation.

Results of such simulations should drive design of support structure and the choice of critical dimensions.

1.4 Summary and Conclusion

Support structure for SLM process is an enabler and a challenge at the same time. They allow for manufacturing of complex designs, but if used inappropriately, they may cause defects in the part, or inefficiencies in the process. By introducing support structure metrics, we proposed a systematic way to evaluate the performance of a support structure. The metrics show that the performance of a support structure is tightly tied to the physics of the SLM process, and designs that ignore this link are often ineffective. Conventional designs provide solutions for most common scenarios, but there is no automated tool for choosing/generating these designs. Therefore, most support structure implementations rely on user experience. Some designs consume less material but are cumbersome to remove, while other designs are the exact opposite.

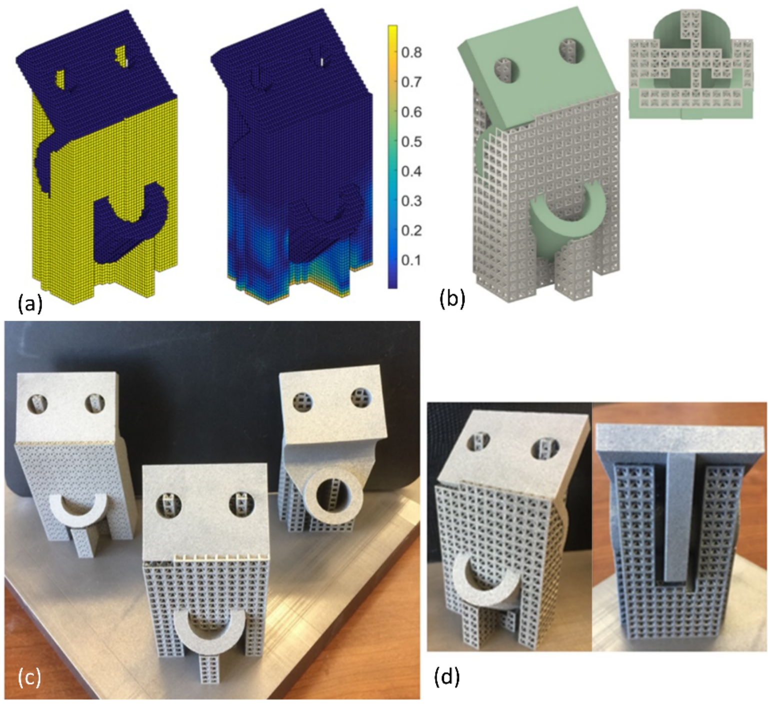

Figure 27: (a) Orientation optimization of maximum residual stress minimization for diagonal lattice structure support [5]. (b) Design reconstruction. (c) Manufactured part and support with different lattice support structures [5]. (d) Different views of the final design [5].

Compromise should be made in utilizing any support structure design based on the metric most relevant to the user.

Future efforts on support structure design for SLM should focus on performance optimization and simulation based, automatic generation. These efforts will eliminate guesswork and inefficiencies. In summary, critical advances in support structure design are needed today to drive the growth and adoption of SLM technology.

Bibliography

[1] Ali, H., Ghadbeigi, H., Mumtaz, K. (2018): Residual stress development in selective laser-melted Ti6Al4V: a parametric thermal modelling approach. Int. J. Adv. Manuf. Technol. Vol. 97, Nr. 5–8, S. 2621–2633.

[2] Buchbinder, D. u. a. (2014): Investigation on reducing distortion by preheating during manufacture of aluminum components using selective laser melting. J. Laser Appl. Vol. 26, Nr. 1, S. 012004.

[3] Calignano, F. (2014): Design optimization of supports for overhanging structures in aluminum and titanium alloys by selective laser melting. Mater. Des. Vol. 64, S. 203–213.

[4] Cheng, L. u. a. (2019): On utilizing topology optimization to design support structure to prevent residual stress induced build failure in laser powder bed metal additive manufacturing. Addit. Manuf. Vol. 27, S. 290–304.

[5] Cheng, L., To, A. (2019): Part-scale build orientation optimization for minimizing residual stress and support volume for metal additive manufacturing: Theory and experimental validation. Comput. Des. Vol. 113, S. 1–23.

[6] Chivel, Y., Smurov, I. (2011): Temperature Monitoring and Overhang Layers Problem. Phys. Procedia. Vol. 12, S. 691–696.

[7] DebRoy, T. u. a. (2018): Additive manufacturing of metallic components – Process, structure and properties. Prog. Mater. Sci. Vol. 92, S. 112–224.

[8] Gan, M.X., Wong, C.H. (2016): Practical support structures for selective laser melting. J. Mater. Process. Technol. Vol. 238, S. 474–484.

[9] Gibson, I., Rosen, D., Stucker, B. (2015): Additive Manufacturing Technologies. Springer New York. New York, NY.

[10] Gusarov, A. V., Kovalev, E.P. (2009): Model of thermal conductivity in powder beds. Phys. Rev. B. Vol. 80, Nr. 2, S. 024202.

[11] Hodge, N.E., Ferencz, R.M., Solberg, J.M. (2014): Implementation of a thermomechanical model for the simulation of selective laser melting. Comput. Mech. Vol. 54, Nr. 1, S. 33–51.

[12] Hussein, A. u. a. (2013): Advanced lattice support structures for metal additive manufacturing. J. Mater. Process. Technol. Vol. 213, Nr. 7, S.

1019–1026.
[13] Järvinen, J.-P. u. a. (2014): Characterization of Effect of Support Structures in Laser Additive Manufacturing of Stainless Steel. Phys. Procedia. Vol. 56, S. 72–81.
[14] Kempen, K. u. a. PRODUCING CRACK-FREE, HIGH DENSITY M2 HSS PARTS BY SELECTIVE LASER MELTING: PRE-HEATING THE BASEPLATE.
[15] King, W. u. a. (2015): Overview of modelling and simulation of metal powder bed fusion process at Lawrence Livermore National Laboratory. Mater. Sci. Technol. Vol. 31, Nr. 8, S. 957–968.
[16] Kuo, Y.-H., Cheng, C.-C., Lin, Y.-S., San, C.-H. (2018): Support structure design in additive manufacturing based on topology optimization. Struct. Multidiscip. Optim. Vol. 57, Nr. 1, S. 183–195.
[17] Langelaar, M. (2016): Topology optimization of 3D self-supporting structures for additive manufacturing. Addit. Manuf. Vol. 12, S. 60–70.
[18] Lefky, C.S. u. a. (2017): Dissolvable Supports in Powder Bed Fusion-Printed Stainless Steel. 3D Print. Addit. Manuf. Vol. 4, Nr. 1, S. 3–11.
[19] Li, Y. u. a. (2018): Modeling temperature and residual stress fields in selective laser melting. Int. J. Mech. Sci. Vol. 136, S. 24–35.
[20] M. Cloots, A.B. Spierings, K.W. (2013): Assessing new support minimizing strategies for the additive manufacturing technology SLM. Solid Freeform Fabrication Symposium (SFF). . Austin, TX. S. 12–14.
[21] Mezzadri, F., Bouriakov, V., Qian, X. (2018): Topology optimization of self-supporting support structures for additive manufacturing. Addit. Manuf. Vol. 21, S. 666–682.
[22] Mirzendehdel, A.M., Suresh, K. (2016): Support structure constrained topology optimization for additive manufacturing. Comput. Des. Vol. 81, S. 1–13.
[23] Mukherjee, T., Zhang, W., DebRoy, T. (2017): An improved prediction of residual stresses and distortion in additive manufacturing. Comput. Mater. Sci. Vol. 126, S. 360–372.
[24] Rombouts, M. u. a. (2005): Photopyroelectric measurement of thermal conductivity of metallic powders. J. Appl. Phys. Vol. 97, Nr. 2, S. 024905.
[25] Schilp, J., Seidel, C., Krauss, H., Weirather, J. (2014): Investigations on Temperature Fields during Laser Beam Melting by Means of Process Monitoring and Multiscale Process Modelling. Adv. Mech. Eng. Vol. 6, S. 217584.
[26] Shiomi, M. u. a. (2004): Residual Stress within Metallic Model Made by Selective Laser Melting Process. CIRP Ann. Vol. 53, Nr. 1, S. 195–198.
[27] Siddique, S. u. a. (2015): Influence of process-induced microstructure and imperfections on mechanical properties of AlSi12 processed by selective laser melting. J. Mater. Process. Technol. Vol. 221, S. 205–213.
[28] Strano, G., Hao, L., Everson, R.M., Evans, K.E. (2013): A new approach to the design and optimisation of support structures in additive manufacturing. Int. J. Adv. Manuf. Technol. Vol. 66, Nr. 9–12, S. 1247–

1254.

[29] Sun, S., Brandt, M., Easton, M. (2017): Powder bed fusion processes. Laser Additive Manufacturing. Elsevier. S. 55–77.

[30] Thijs, L. u. a. (2010): A study of the microstructural evolution during selective laser melting of Ti–6Al–4V. Acta Mater. Vol. 58, Nr. 9, S. 3303–3312.

[31] Vanek, J., Galicia, J.A.G., Benes, B. (2014): Clever Support: Efficient Support Structure Generation for Digital Fabrication. Comput. Graph. Forum. Vol. 33, Nr. 5, S. 117–125.

[32] Wang, D., Yang, Y., Yi, Z., Su, X. (2013): Research on the fabricating quality optimization of the overhanging surface in SLM process. Int. J. Adv. Manuf. Technol. Vol. 65, Nr. 9–12, S. 1471–1484.

[33] Wei, C. u. a. (2019): Easy-To-Remove Composite Support Material and Procedure in Additive Manufacturing of Metallic Components Using Multiple Material Laser-Based Powder Bed Fusion. J. Manuf. Sci. Eng. Vol. 141, Nr. 7, S. 071002.

[34] Wohlers, T., Caffrey, T. (2014): Wohlers Report 2014 - 3D Printing and Additive Manufacturing State of the Industry. Anual Worldwide Progress Report.

[35] Wu, Y.-C. u. a. (2018): Numerical modeling of melt-pool behavior in selective laser melting with random powder distribution and experimental validation. J. Mater. Process. Technol. Vol. 254, S. 72–78.

[36] Yadroitsev, I., Bertrand, P., Smurov, I. (2007): Parametric analysis of the selective laser melting process. Appl. Surf. Sci. Vol. 253, Nr. 19, S. 8064–8069.

[37] Yadroitsev, I., Gusarov, A., Yadroitsava, I., Smurov, I. (2010): Single track formation in selective laser melting of metal powders. J. Mater. Process. Technol. Vol. 210, Nr. 12, S. 1624–1631.

[38] Yang, Y., Gu, D., Dai, D., Ma, C. (2018): Laser energy absorption behavior of powder particles using ray tracing method during selective laser melting additive manufacturing of aluminum alloy. Mater. Des. Vol. 143, S. 12–19.

[39] Zhang, Z. u. a. (2018): Design of internal branch support structures for selective laser melting. Rapid Prototyp. J. S. 00–00.

[40] Zhao, X. u. a. (2009): The effect of hot isostatic pressing on crack healing, microstructure, mechanical properties of Rene88DT superalloy prepared by laser solid forming. Mater. Sci. Eng. A. Vol. 504, Nr. 1–2, S. 129–134.

[41] e-Stage Metal | 3D Printing Software, https://www.materialise.com/en/software/e-stage/product-information-metal, (27.06.2019).

[42] Materialise Magics, https://www.materialise.com/en/software/magics, (09.07.2018).

[43] (2011): Selective Laser Melting, https://en.wikipedia.org/wiki/Selective_laser_melting.